

# Improved GPS data analysis strategy for tide gauge benchmark monitoring

Alvaro Santamaría-Gómez

Instituto Geográfico Nacional, c/ General Ibañez Ibero 3, 28071, Madrid, Spain

Institut Géographique National, LAREG/GRGS, 6 - 8 av. Blaise Pascal, 77455, Champs-sur-Marne, France

Marie-Noëlle Bouin

Institut Géographique National, LAREG/GRGS, 6 - 8 av. Blaise Pascal, 77455, Champs-sur-Marne, France

CNRM/CMM, Météo France, 13 rue du Chatellier, CS 12804, 29228 Brest, France

Guy Wöppelmann

Université de La Rochelle-CNRS, UMR 6250 LIENSS, 2 rue Olympe de Gouges, 17000, La Rochelle, France

**Abstract.** The University of La Rochelle (ULR) TIGA Analysis Center (TAC) completed a new global reprocessed solution spanning 13 years with more than 300 GPS permanent stations, 216 of them being co-located with tide gauges. A state-of-the-art GPS processing strategy was applied, in particular, the station sub-networks used in the daily processing were optimally built. Station vertical velocities were estimated in the ITRF2005 reference frame by stacking the weekly position estimates. Outliers, offsets and discontinuities in time series were carefully examined. Vertical velocities uncertainties were assessed in a realistic way by analysing the type and amplitude of the noise content in the residual position time series. The comparison shows that the velocity uncertainties have been reduced by a factor of 2 with respect to previous ULR solutions. The analysis of this solution and its by-products shows the high geodetic quality achieved in terms of homogeneity, precision and consistency with respect to other top-level geodetic solutions.

**Keywords:** GPS, tide gauges, ITRF.

---

## 1 Introduction

In order to estimate long-term geocentric sea level rise, tide gauges trends must be corrected for the long-term vertical displacements of the land upon which they are settled. In addition, for proper satellite altimeter calibration purposes, tide gauges trends must be referred to a common, global and stable reference frame, such as the latest realization of the International Terrestrial Reference Frame (ITRF) [Altamimi et al., 2007].

These long-term vertical displacements can be corrected by modelling geological processes as the Global Isostatic Adjustment (GIA) [e.g. Douglas, 2001] or directly from continuous geodetic observations at or near tide gauges. This second method

should be preferred as it takes into account local displacements (geological, anthropogenic or whatever), not accounted for in the GIA models. Within the different geodetic techniques used for this purpose (GPS, DORIS and absolute gravity), GPS is the most widespread. Recent studies [Wöppelmann et al., 2009; Bouin and Wöppelmann, 2010] have shown that correcting the tide gauge trends using continuous GPS stations (cGPS@TG) improves the consistency of the sea level rates. To this aim, the International GNSS Service (IGS) Tide Gauge Benchmark Monitoring Pilot Project (TIGA) was established in 2001 [Schöne et al., 2009]. Since 2002, the ULR consortium contributes to the TIGA project as an Analysis and Data Center [Wöppelmann et al., 2004].

Several global vertical velocity field solutions (ULR solutions hereafter) were released with different station networks, time spans and processing strategies [Wöppelmann et al., 2007; 2009]. In this paper, we present the fourth ULR solution based on an homogeneous reprocessing of a larger global network of 316 stations, spanning an increased period of 13 years (January 1996 to December 2008). This solution comes out with a new data analysis strategy, including a new sub-network design and combination. The troposphere and ocean tide modelisation were also improved. Both GPS processing and vertical velocity estimation strategies are described; realistic uncertainties are estimated by analysing the noise content of time series. Finally, the quality of the solution is assessed and discussed.

## 2 Data analysis strategy

### 2.1 Data

The global tracking network consists of 316 GPS stations. 216 of them are cGPS@TG, including 81 stations committed to TIGA. Also 124 of them are IGS reference frame (RF) stations used for realizing the reference frame [Kouba et al., 1998] and for improving the network geometry.

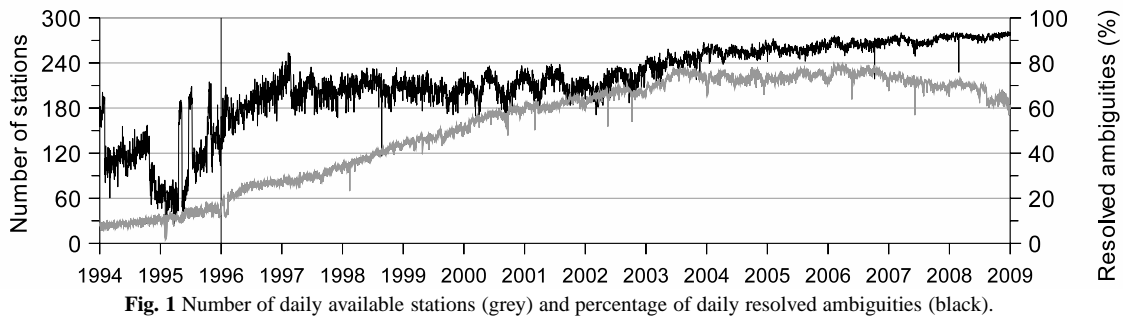


Fig. 1 Number of daily available stations (grey) and percentage of daily resolved ambiguities (black).

This network was processed over the period 1st January 1994 to 31st December 2008. Small RINEX files (less than 5 hours of observation) were rejected. This quality check procedure yielded a number of daily available stations between a minimum of 25 in 1994 (53 in 1996) and a maximum of 239 in 2006 (grey line in Figure 1). 1994 and 1995 were finally not retained in the solution due to a lack of fixed ambiguities and therefore quality (black line in Figure 1) and they will not be further considered.

## 2.2 Improved network geometry

GPS processing time increases exponentially with the number of stations. To overcome this limitation, it is usual to split the whole network in several sub-networks, to process each sub-network independently and then to combine the sub-network solutions into a unique daily solution.

Historic ULR solutions (ULR1 to ULR3 solutions) used five global, manually-selected, permanent sub-networks over the entire data span (“static sub-networks” hereafter). Using this approach, the a priori stations included in each sub-network were always the same, whether or not their data were available for a specific day, making the geometry worse when their data were missing, and therefore, possibly yielding an unnecessary large number of sub-networks in the processing (always five). This static configuration was changed in the ULR4 solution into a new station distribution approach resulting in global, automatic, daily-variable sub-networks (“dynamic sub-networks” hereafter), with up to 50 stations per sub-network.

Shorter baselines improves ambiguity resolution [Steigenberger et al., 2006]. With the dynamic approach, all daily available stations were distributed into the strictly necessary number of sub-networks, ensuring optimal dense sub-networks. Thus, the number of dynamic sub-networks used grows from 1 in 1996 to 6 in 2003. Moreover, to obtain global geometrically well-distributed sub-networks for optimal orbit estimation, each station is assigned to the sub-network where it is more isolated, i.e. reducing the baselines. In this way, “deserted” areas of each sub-network are iteratively being “populated”.

In addition, six daily-variable common IGS RF stations, with more than 12h of observation, are included in each dynamic sub-network to combine the solutions. Northernmost and southernmost stations are always selected and then four other globally well-distributed stations are added.

Static versus dynamic approaches were compared by processing two solutions using the same stations and processing strategy except for the stations distribution. Figure 2 shows that using dynamic sub-networks clearly increases the percentage of resolved ambiguities as the number of available stations decreases, up to 20% in 1997 (Figure 2). The 10% offset in the percentage of resolved ambiguities observed at the end of 1999 for both approaches is related to the use of code bias corrections (see section 2.3), only available for post-2000 year period when the test was performed.

## 2.3 Models and parameterization

Double-differenced ionosphere-free carrier phase data is analysed using GAMIT software version 10.34 [Herring et al., 2006a]. The elevation cut-off angle is set to  $10^\circ$ , avoiding mismodelling of low-elevation troposphere and phase center variations (PCV) of relative-to-absolute antenna calibration. Sampling rate is set to 3 minutes. Carrier phase observations are weighted in two iterations: by elevation angle first and then by elevation angle and by station, accounting for the station phase residuals

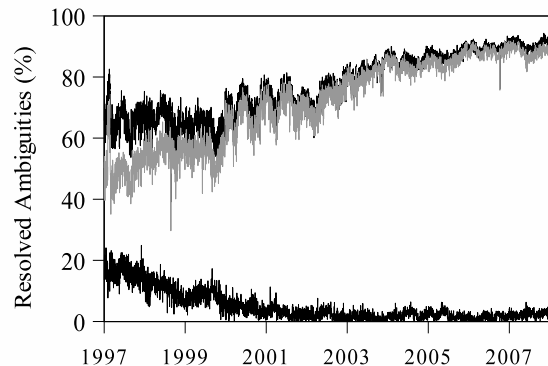


Fig. 2 Resolved ambiguities for static (grey), dynamic sub-networks (top black) and the difference (bottom black).

from the first iteration. Code bias corrections are applied for the whole period using monthly tables from the Astronomical Institute of the University of Bern (AIUB) [IGSMail-2827 (2000) at <http://igs.cb.jpl.nasa.gov/mail/>]. Real-valued double differenced phase cycle ambiguities are adjusted except when they can be resolved confidently. In this case, they are fixed using the Melbourne-Wübbena wide-lane to resolve L1-L2 cycles and then estimation to resolve L1 and L2 cycles. For satellite antennas, satellite-specific z-offsets [Ge et al., 2005] and block-specific nadir angle-dependent absolute PCV [Schmid et al., 2007] are applied. For receiver antennas, L1/L2 offsets and azimuth-dependent, when available, and elevation-dependent absolute PCV are applied. A priori zenith hydrostatic (dry) delay values are extracted by station from the ECMWF meteorological model through the VMF1 grids [Boehm et al., 2006]. Residual delays are adjusted for each station assuming mostly dominated by the wet component and parameterized by a piecewise linear, continuous model with 2 hour intervals. Both dry and wet VMF1 mapping functions are used. One gradient is estimated for each day and each station. Solid Earth tides are corrected following IERS Conventions (2003) [McCarthy and Petit, 2004]. Ocean tide loading is corrected using FES2004 model [Lyard et al., 2006]. No atmospheric tide nor non-tidal corrections were applied. Earth orientation parameters (EOP) are daily estimated as a piecewise, linear model with a priori values from IERS Bulletin B. UT1-UTC offsets are highly constrained to their a priori values. Satellite positions and velocities are adjusted in 24 hours arcs taking IGS final orbits [Dow et al., 2005] as a priori. Solar radiation pressure parameters are estimated using the Berne model [Beutler et al., 1994].

## 2.4 Data processing scheme and reference frame

Each dynamic sub-network is processed independently using GAMIT software. The daily sub-network solutions are combined into a daily solution (by estimating only translations and rotations) using GLOBK [Herring et al., 2006b] by means of the estimated orbital parameters, the estimated positions of the six common stations and their estimated zenith tropospheric path delays. Daily loose solutions are constrained by no-net-rotation (NNR) constraints with respect to ITRF2005 and combined into a weekly solution using CATREF software [Altamimi et al., 2007]. These weekly solutions are aligned to ITRF2005 using NNR constraints with all IGS RF stations available, whereas inner constraints [Altamimi et al., 2007] are used for scale and translation, in order to preserve the weekly apparent geocenter motion information.

All the weekly solutions for the whole period (GPS weeks 0834 to 1512), are then combined into a long-term solution using CATREF. This long-term solution (ULR4) is aligned to ITRF2005 using minimal constraints over all the transformation parameters with a selected set of IGS RF stations called datum. The 68 stations retained in the datum were selected based on their data availability (at least present in 80% of the whole processed period) and their quality as follows. Firstly, stations with known or suspected velocity discontinuities were rejected, and secondly, in an iterated process, stations showing large position and velocity residuals with respect to ITRF2005 values were also rejected. Thresholds for positions were set to 0.5 cm in horizontal and 1.5 cm in vertical. The larger value in the vertical component is due to the fact that ITRF2005 GPS coordinates were estimated with a relative PCV model. Station differences using the absolute PCV model are estimated to be within this range. Thresholds for velocity residuals were set to 1.5 mm/yr and 2 mm/yr respectively.

The residual position time series of each station were visually examined. To avoid biased velocities, all discontinuities (significant offsets and velocity changes) were detected, identified if possible, and removed using ITRF2005 discontinuities as a priori. Then, all outliers were removed in an iterative process, from bigger to smaller magnitude (depending on the time series noise), down to a minimum of 2 cm for residuals and 4 for normalized residuals.

## 3 Results

### 3.1 Vertical rates

The vertical velocity fields of ULR4 and ULR3 [Wöppelmann et al., 2009] solutions were compared using a common set of 170 stations with more than 4.5 years of data. Figure 3 shows that most of the velocity differences are below 1 mm/yr (RMS of 0.8 mm/yr), except some stations for which larger differences are due to different discontinuities on their

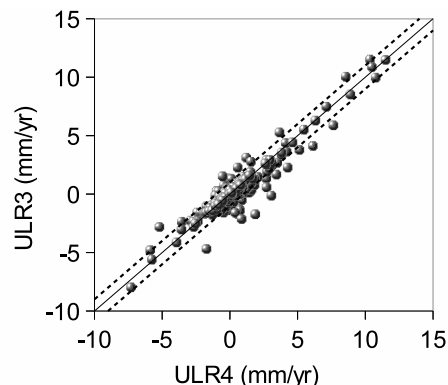


Fig. 3 Vertical velocity difference between ULR3 and ULR4. Dashed lines represent  $\pm 1$  mm/yr.

time series. The mean difference between both velocity fields is  $0.16 \pm 0.06$  mm/yr which is related to the different datum used to align the solutions. This misalignment is under the internal precision of the ITRF2005.

From the complete ULR4 solution, 224 stations with more than 4.5 years of data were retained. For these stations, their estimated velocities are confidently not influenced by seasonal signals [Blewitt and Lavallée, 2002]. Nevertheless, the rate uncertainties estimated with a standard least squares algorithm (based on a Gaussian white noise process) are clearly optimistic by a factor of 3-11 [Zhang et al., 1997; Mao et al., 1999]. More realistic uncertainties of the estimated velocities must account for correlated noise present in the time series.

A noise analysis was performed using the Maximum Likelihood Estimation (MLE) technique (CATS software, [Williams, 2008]). Vertical velocity uncertainties were estimated using a white noise plus power law noise model. To avoid biased adjustments, time series were previously examined for periodic signals. Besides the annual and semi-annual terms, we also found and removed up to six harmonics of the GPS “draconitic” period described by Ray et al., 2007. Figure 4 shows the histogram of the realistic vertical velocity uncertainties of the ULR4 solution with respect to the realistic uncertainties estimated for the ULR3 solution also using CATS. The improvement is close to a factor of 2. Also the factor of optimism of the formal uncertainties with respect to the realistic ones is 2-3, quite smaller than the above-mentioned values. This is due to the improvement and consistency of the processing strategy presented here, which results in a noticeable reduction of the correlated noise content for the ULR4 solution compared to previous solutions.

### 3.2 Weekly repeatability

The internal quality of the ULR4 solution was assessed by analysing the repeatability of the weekly position solutions. Figure 5 shows the repeatability

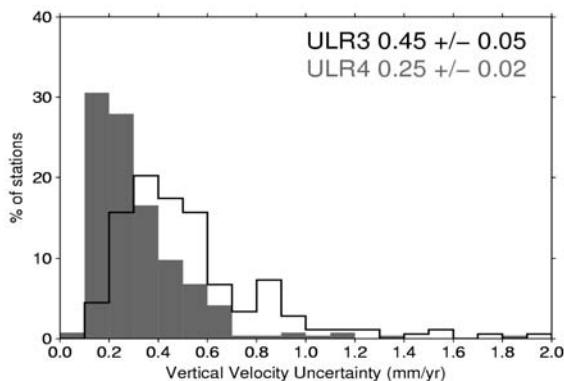


Fig. 4 Histogram of estimated uncertainties for ULR4 (grey) and ULR3 (black) solutions and their median values.

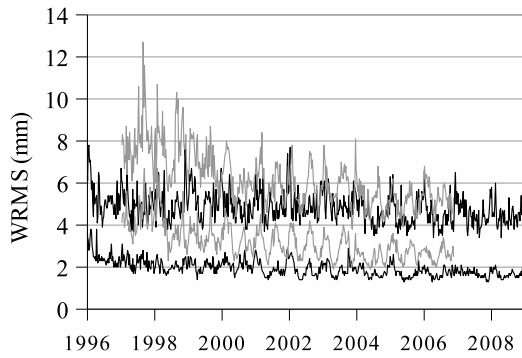


Fig. 5 Horizontal (bottom) and vertical (top) weighted RMS of the weekly solutions with respect to the long-term solution for both ULR4 (black) and ULR3 (grey) solutions.

of the time series (mean values of the weighted RMS of the weekly positions with respect to the long-term combined positions) for ULR4 and ULR3 solutions. Horizontal and vertical repeatabilities are improved in the ULR4 solution. Moreover, for the whole reprocessed period vertical repeatabilities are more stable, showing the improved ULR4 time consistency. ULR4 repeatability values are between 1 and 3 mm for the horizontal and between 4 and 6 mm for the vertical component (3D weighted RMS between 2 and 4 mm). These values are fully consistent with those of the IGS combined solution [Altamimi and Collilieux, 2008], showing that ULR4 solution is comparable in quality with the ITRF2005.

### 3.3 Origin and scale

As a satellite technique, GPS estimated origin should be coincident with the Earth’s center of mass. However this affirmation is not completely fulfilled due to remaining GPS-specific systematic errors, as the modelling of the solar radiation pressure coefficients or the unaccounted effect of higher ionospheric orders [Hernández-Pajares et al., 2007].

We have estimated here apparent geocenter motion using the network shift or geometric approach [Lavallée et al., 2006]. Figure 6 shows the translation and scale parameters of the weekly solutions with respect to the long-term combined solution aligned to the ITRF2005. Translation trends are not significant, showing the consistency of the secular origin definition with respect to the ITRF2005. The scale shows no trend either, as this parameter is completely dependent on the ITRF2005 scale definition through the satellites antenna z-offset corrections. For intercomparison purposes, an annual signal was estimated for each transformation parameter (Table 1).

Compared to SLR results [Collilieux et al., 2009], the annual amplitudes of the equatorial components (X and Y) and the scale are fully consistent. However, the amplitude of the Z component is twice larger. Regarding the annual phase, the scale

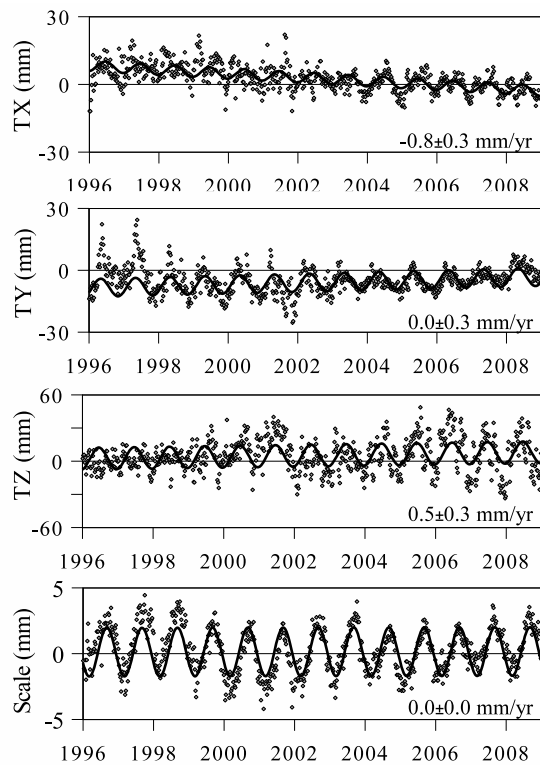


**Fig. 6** Weekly translation and scale parameters with respect to the ITRF2005. Also their trends and annual signal are traced.

**Table 1.** Annual signal of apparent geocenter and scale

	Amplitude (mm)	Phase (deg)
TX	$2.3 \pm 0.2$	$164.6 \pm 5.4$
TY	$4.2 \pm 0.3$	$122.2 \pm 3.5$
TZ	$9.9 \pm 0.8$	$171.3 \pm 3.5$
Scale	$1.8 \pm 0.1$	$243.2 \pm 1.6$

parameter is fully consistent, but all translational parameters show a shift of about  $137^\circ$  (4.5 months). Compared to other GPS results [Lavallée et al., 2006], the amplitude of the Z component and both equatorial phases are consistent. The phase of Z component exhibits larger solution-dependent variations. Both issues point probably at the above-mentioned GPS systematic errors and also at the poor performance of the network shift method used with a not-well distributed global network [Lavallée et al., 2006].

### 3.4 Orbits

The estimated ULR4 orbits were compared with the current official non-reprocessed IGS final orbits [Dow et al., 2005]. A classic 7-parameter Helmert transformation was applied between both 24h-arc sets. 1D RMS differences (the average of the three RMS components) were estimated for each common observed satellite and then the median daily RMS value was extracted and traced (black line, Figure 7).

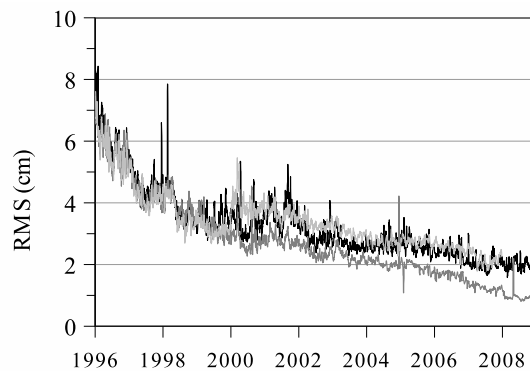


**Fig. 7** 7-day smoothed daily RMS between final IGS orbits and ULR (black), SIO/SOPAC (light grey) and CODE/AIUB (dark grey) reprocessed orbits.

We show that ULR and IGS orbits are in good agreement with each other, from 8.5 cm in 1996 to 1.5 cm in 2009. The same range of differences was obtained between IGS orbits and reprocessed orbits from SIO/SOPAC IGS Analysis Center (light grey line). Some smaller differences were obtained with reprocessed CODE/AIUB IGS Analysis Center (dark grey line) for the post-2000 period. This demonstrates that the ULR4 orbits are of the same quality as the reprocessed orbits of some of the IGS Analysis Centers.

## 4 Concluding remarks

The new ULR4 solution is based on an homogeneous reprocessing of a global GPS network of 316 stations spanning up to 13 years of data. The processing strategy was improved with respect to past ULR solutions. Special attention was paid to the sub-network geometry distribution, which clearly improves the quality of the reprocessing by increasing the number of resolved ambiguities. The analysis of the results and by-products of this solution (vertical velocities, repeatability, transformation parameters and orbits) shows the high geodetic quality achieved. The state-of-the-art GPS processing strategy implemented fulfils the IGS requirements and recommendations. Thereby, in addition to the IGS TIGA project, the ULR consortium is participating with its latest solution to the first IGS reanalysis campaign, enabling an invaluable extension of IGS and ITRF reference frames towards tide gauges. Also, the ULR consortium is contributing to the Working Group on Regional Dense Velocity Fields of the International Association of Geodesy Subcommission 1.3. [Bruyninx, submitted, this issue]. Further studies will be carried out in order to assess the geophysical usefulness of this solution. For example, this global and accurate vertical velocity field may be used to separate vertical land motion trends from relative sea level trends as recorded by tide gauges.

**Acknowledgements.** The authors acknowledge two unknown reviewers who contributed to an improved paper. We also thank the invaluable technical support given by Mikael Guichard, Marc-Henri Boisis-Delavaud and Frederic Bret from the IT centre of the University of La Rochelle (ULR). The ULR computing infrastructure used for the reprocessing of the GPS data was partly funded by the European Union (Contract 31031-2008, European regional development fund). This work was also feasible thanks to all institutions and individuals worldwide that contribute to make GPS data and products freely available.

## References

- Altamimi, Z. and Collilieux, X. (2008). IGS contribution to ITRF. *J. Geod.*, 83(3-4):375–383.
- Altamimi, Z., Collilieux, X., Legrand, J., Garayt, B., and Boucher, C. (2007). ITRF2005: A new release of the International Terrestrial Reference Frame based on time series of station positions and Earth Orientation Parameters. *J. Geophys. Res.*, 112(B09401).
- Beutler, G., Brockmann, E., Gurtner, W., Hugentobler, U., Mervart, L., and Rothacher, M. (1994). Extended orbit modeling techniques at the CODE Processing Center of the International GPS Service for Geodynamics (IGS): theory and initial results. *Manuscripta Geodaetica*, (19):367–386.
- Blewitt, G. and Lavallée, D. (2002). Effect of annual signals on geodetic velocity. *J. Geophys. Res.*, 107(B02145).
- Boehm, J., Werl, B., and Schuh, H. (2006). Troposphere mapping functions for GPS and very long baseline interferometry from European Centre for Medium-Range Weather Forecasts operational analysis data. *J. Geophys. Res.*, 111(B02406).
- Bouin, M.-N. and Wöppelmann, G. (2010). Land motion estimates from GPS at tide gauges: a geophysical evaluation. *Geophys. J. Int.*, (180):193–209.
- Bruyninx, C. e. a. A dense global velocity field based on GNSS observations: preliminary results. *Submitted, this issue*.
- Collilieux, X., Altamimi, Z., Ray, J., van Dam, T., and Wu, X. (2009). Effect of the satellite laser ranging network distribution on geocenter motion estimation. *J. Geophys. Res.*, 114(B02145).
- Douglas, B. (2001). *Sea level change in the era of the recording tide gauge*, volume 75 of *International Geophysics Series*. Academic, San Diego, California.
- Dow, J. M., Neilan, R. E., and Gendt, G. (2005). The International GPS Service: Celebrating the 10th anniversary and looking to the next decade. *Adv. Space Res.*, 36:320–326.
- Ge, M., Gendt, G., Dick, G., Zhang, F., and Reigber, C. (2005). Impact of GPS satellite antenna offsets on scale changes in global network solutions. *Geophys. Res. Lett.*, 32(L06310).
- Hernández-Pajares, M., Juan, J. M., Sanz, J., and Orús, R. (2007). Second-order ionospheric term in GPS: Implementation and impact on geodetic estimates. *J. Geophys. Res.*, 112(B08417).
- Herring, T. A., King, R. W., and McClusky, S. C. (2006a). GAMIT: Reference Manual Version 10.34. *Internal Memorandum, Massachusetts Institute of Technology, Cambridge*.
- Herring, T. A., King, R. W., and McClusky, S. C. (2006b). GLOBK: Global Kalman filter VLBI and GPS analysis program Version 10.3. *Internal Memorandum, Massachusetts Institute of Technology, Cambridge*.
- Kouba, J., J.R., R., and Watkins, M. (1998). IGS Reference Frame realization. IGS 1998 Analysis Center Workshop - Proceedings Darmstadt. page 139.
- Lavallée, D., van Dam, T., Blewitt, G., and Clarke, P. (2006). Geocenter motions from GPS: A unified observation model. *J. Geophys. Res.*, 111(B05405).
- Lyard, F., Lefevre, F., Letellier, T., and Francis, O. (2006). Modelling the global ocean tides: modern insights from FES2004. *Ocean Dynamics*, 56:394–415.
- Mao, A., Harrison, C. G. A., and Dixon, T. H. (1999). Noise in GPS coordinate time series. *J. Geophys. Res.*, 104:2797–2816.
- McCarthy, D. and Petit, G. (2004). IERS Technical Note 32 - IERS Conventions (2003). Technical report, Verlag des Bundesamts für Kartographie und Geodäsie, Frankfurt am Main, Germany.
- Ray, R., Altamimi, Z., Collilieux, X., and Van Dam, T. (2007). Anomalous harmonics in the spectra of GPS position estimates. *GPS Solutions*, 12(1):55–64.
- Schmid, R., Steigenberger, P., Gendt, G., Ge, M., and Rothacher, M. (2007). Generation of a consistent absolute phase-center correction model for GPS receiver and satellite antennas. *J. Geod.*, 81:781–798.
- Schöne, T., Schön, N., and Thaller, D. (2009). IGS Tide Gauge Benchmark Monitoring Pilot Project (TIGA): scientific benefits. *J. Geod.*, 83:249–261.
- Steigenberger, P., Rothacher, M., Dietrich, R., Fritsche, M., Rülke, A., and Vey, S. (2006). Reprocessing of a global GPS network. *J. Geophys. Res.*, 111(B05402).
- Williams, S. D. P. (2008). CATS: GPS coordinate time series analysis software. *GPS Solutions*, 12(2):147–153.
- Wöppelmann, G., Letretel, C., Santamaría, A., Bouin, M.-N., Collilieux, X., Altamimi, Z., Williams, S., and Martín Míguez, B. (2009). Rates of sea-level change over the past century in a geocentric reference frame. *Geophys. Res. Lett.*, 36(L12607).
- Wöppelmann, G., Martín Míguez, B., Bouin, M.-N., and Altamimi, Z. (2007). Geocentric sea-level trend estimates from GPS analyses at relevant tide gauges world-wide. *Global and Planetary Change*, 57(3-4):396–406.
- Wöppelmann, G., McLellan, S., Bouin, M.-N., Altamimi, Z., and Daniel, L. (2004). Current GPS data analysis at CLDG for the IGS TIGA Pilot Project. *Cahiers du Centre Européen Géodynamique & de Sismologie*, 23:149–154.
- Zhang, J., Bock, Y., Johnson, H., Fang, P., Williams, S., Genrich, J., Wdowinski, S., and Behr, J. (1997). Southern California Permanent GPS Geodetic Array: Error analysis of daily position estimates and site velocities. *J. Geophys. Res.*, 102:18035–18056.